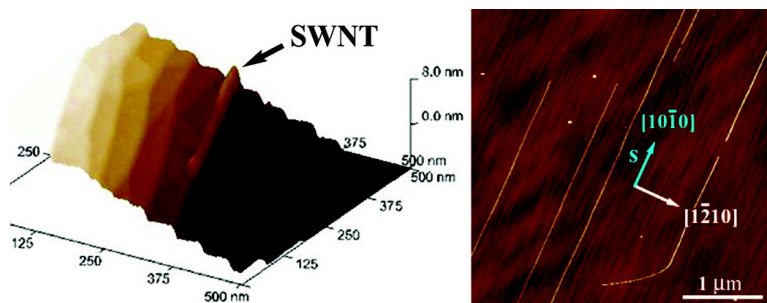


Carbon Nanotube Graphoepitaxy: Highly Oriented Growth by Faceted Nanosteps

Ariel Ismach, David Kantorovich, and Ernesto Joselevich

J. Am. Chem. Soc., **2005**, 127 (33), 11554-11555 • DOI: 10.1021/ja052759m • Publication Date (Web): 30 July 2005

Downloaded from <http://pubs.acs.org> on March 25, 2009



More About This Article

Additional resources and features associated with this article are available within the HTML version:

- Supporting Information
- Links to the 17 articles that cite this article, as of the time of this article download
- Access to high resolution figures
- Links to articles and content related to this article
- Copyright permission to reproduce figures and/or text from this article

[View the Full Text HTML](#)



Carbon Nanotube Graphoepitaxy: Highly Oriented Growth by Faceted Nanosteps

Ariel Ismach, David Kantorovich, and Ernesto Joselevich*

Department of Materials and Interfaces, Weizmann Institute of Science, Rehovot 76100, Israel

Received April 28, 2005; E-mail: ernesto.joselevich@weizmann.ac.il

Carbon nanotubes have unique properties, which make them potentially useful building blocks for nanoelectronics,¹ but their organization into horizontal arrays on surfaces remains a critical issue for large-scale integration. In-plane directional growth of single-wall carbon nanotubes has been achieved by electric fields,² gas flow,³ lattice directions,⁴ and atomic steps.⁵ Epitaxy on periodically faceted surfaces has been extensively used for the nonlithographic production of self-assembled nanowire arrays.⁶ However, this approach has not yet been extended to carbon nanotubes. Graphoepitaxy, in contrast to the more classical commensurate epitaxy, usually refers to the incommensurate orientation of crystals⁷ or periodic molecular assemblies⁸ by relief features of the substrate, such as steps or grooves, which can be significantly larger than the lattice parameter. Here we report for the first time the oriented growth of carbon nanotubes on periodically faceted surfaces. Discrete single-wall carbon nanotubes (SWNTs) form in graphoepitaxy along faceted nanosteps, which had spontaneously self-assembled on the surface of annealed miscut C-plane sapphire. Depending on the miscut orientation and annealing conditions, graphoepitaxy leads to the formation of either unprecedentedly straight and parallel nanotubes, with angular deviations as small as $\pm 0.5^\circ$, or to wavy nanotubes loosely conformal to sawtooth-shaped faceted nanosteps.

The procedures and models for the different morphologies of graphoepitaxial nanotubes are flowcharted in Figure 1, and

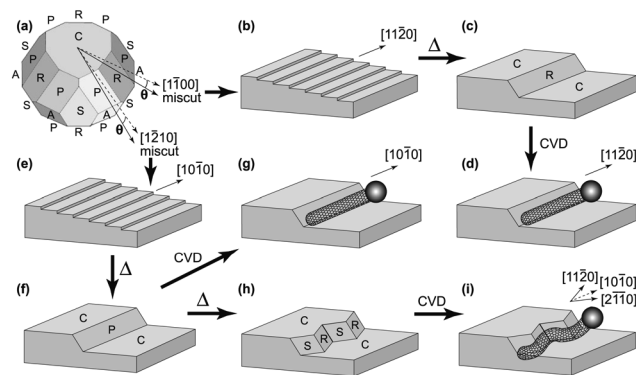


Figure 1. Flowchart describing the formation of possible morphologies of carbon nanotube graphoepitaxy by miscut of C-plane sapphire, annealing, and CVD. (a) Equilibrium shape of α -Al₂O₃, with facets C{0001}, R{1102}, S{1011}, P{1123}, and A{1120}, in order of increasing surface energy. The same drawing is used to show the different miscut directions. (b) Miscut toward [1100] produces a vicinal α -Al₂O₃ (0001) surface with atomic steps along [1120]. (c) Annealing leads to R-faceted nanosteps. (d) SWNTs grow straight along [1120] (the ball represents the catalyst nanoparticle). (e) Miscut toward [1210] produces a vicinal α -Al₂O₃ (0001) with atomic steps along [1010]. (f) Annealing initially leads to metastable P-faceted nanosteps. (g) SWNTs grow straight along [1010]. (h) Further annealing from (f) leads to sawtooth-shaped S-/R-faceted nanosteps. (i) SWNTs grow loosely conformal to the sawtooth-shaped nanosteps, with segments along [1120] and [2110].

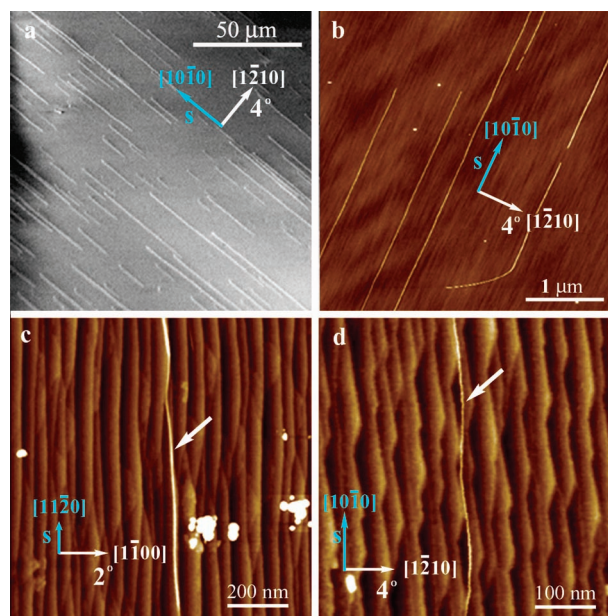


Figure 2. Graphoepitaxial SWNTs on different annealed miscut C-plane sapphire. (a) Straight nanosteps along [1010], as in Figure 1g, observed by SEM. (b) AFM image of (a), showing the nanosteps. (c) Nanosteps along [1120], as in Figure 1d. (d) Highly faceted sawtooth-shaped nanosteps along [1010], as in Figure 1i.

representative results are shown in Figure 2 (experimental details and additional figures are available as Supporting Information).

Different substrates were produced as wafers by cutting and mechanically polishing single crystals of sapphire (α -Al₂O₃) at 2° or 4° off the C-plane toward the [1100] or [1210] directions (Figure 1a). The lattice and miscut orientations were determined by a previously described technique of asymmetric double-exposure back-reflection X-ray diffraction.⁵ The substrates were then thermally annealed at 1100 °C in air for 5–10 h. The SWNTs were grown from C₂H₄ and Fe nanoparticles by chemical vapor deposition (CVD) at 800 °C, as previously described.^{2,5}

The faceting tendencies of sapphire are indicated by its equilibrium shape⁹ (Figure 1a), where the relative area of the different facets decreases with their surface energy. Miscut toward [1100] at room temperature produces vicinal α -Al₂O₃ (0001) surfaces with atomic steps along [1120] (Figure 1b), whereas miscut toward [1210] produces atomic steps along [1010] (Figure 1e). For consistency, we define the step direction by a step vector⁵ $\mathbf{s} = \hat{\mathbf{c}} \times \hat{\mathbf{n}}$, where $\hat{\mathbf{c}}$ and $\hat{\mathbf{n}}$ are unit vectors normal to the C-plane and to the surface plane, respectively, so that \mathbf{s} is parallel to the steps, descending to the right. Upon annealing, the thermodynamically unstable atomic steps tend to reduce the surface energy by bunching together into faceted nanosteps spaced by flat C-plane terraces.¹⁰ The size of the faceted nanosteps is determined by equilibrium between the elastic energy due to surface stress and the energy of

the facet edges. Following Marchenko theory,^{6,11} the energy of a periodically faceted vicinal surface per unit of horizontal area is given by eq 1, where γ_0 and γ_1 are the surface energies of the flat terrace and the step facet, respectively, H and D are the step height and spacing, respectively, η is the energy of the facet edges, τ is the intrinsic surface stress, Y is the Young's modulus, a is the lattice parameter, and C_1 and C_2 are geometric factors related to the symmetry and elastic anisotropy of the facets. Upon annealing, the steps reach an equilibrium height H_{eq} when $\partial E/\partial H = 0$. Considering that H and D are related to the miscut inclination θ (Figure 1a) by $H/D \approx \theta$, this leads to eq 2, which explains the self-assembly of steps with heights that can be about 3 times or greater than the lattice parameter. Since H_{eq} is independent of θ , the step spacing D is inversely proportional to θ .

$$E = \gamma_0 + \gamma_1 \frac{H}{D} + \frac{C_1 \eta}{D} - \frac{C_2 \tau^2}{YD} \ln\left(\frac{H}{a}\right) \quad (1)$$

$$H_{\text{eq}} = a \exp\left(1 + \frac{C_1 \eta Y}{C_2 \tau^2}\right) \quad (2)$$

The faceted nanosteps observed after annealing vicinal $\alpha\text{-Al}_2\text{O}_3$ (0001)¹⁰ indeed have heights between 1 and 3 times larger than the unit cell, i.e., $H_{\text{obs}} = c - 3c = 1.3\text{--}3.8$ nm, resulting from the bunching of 6–18 atomic steps⁵ of height $h = c/6 = 0.21$ nm. In equilibrium, the facet of the nanostep should be the most stable facet of $\alpha\text{-Al}_2\text{O}_3$ (Figure 1a) that follows the macroscopic surface plane. Thus, the atomic steps along $[1\bar{1}20]$ (Figure 1b) can bunch into stable R-faceted nanosteps (Figure 1c), and nanotubes grown on this surface graphoepitaxially form along the $[1\bar{1}20]$ direction (Figure 1d), as experimentally observed in Figure 2c. Following the same principle, the atomic steps along $[10\bar{1}0]$ (Figure 1e) initially bunch into P-faceted nanosteps (Figure 1f), which lead to graphoepitaxial nanotubes along $[10\bar{1}0]$, observed in a and b of Figure 2. However, since the P facet has a large surface energy, these P-faceted nanosteps are metastable, and upon further annealing, they break into sawtooth-shaped S/R-bifaceted nanosteps (Figure 1h). Due to the stiffness of the nanotubes and their relatively weak interaction with the faceted surface, graphoepitaxy produces nanotubes loosely conformal to alternate S and R facets along $[1\bar{1}20]$ and $[2\bar{1}10]$, respectively, as observed in Figure 2d. Curiously, the most strikingly straight and parallel nanotubes (Figure 2a,b), with angular deviations as small as $\pm 0.5^\circ$, are obtained on the metastable nanosteps along $[10\bar{1}0]$ before their breakdown. This may be attributed to the relatively high surface energy of the P facet, which could stabilize via the interaction with the growing nanotubes and catalyst nanoparticles.

A topographic 3D projection and a section analysis of graphoepitaxial SWNTs on faceted nanosteps are shown in Figure 3. The height of the nanosteps corresponds to one unit cell, $c = 1.3$ nm. The nanotube has a slightly larger height, and is located next to the nanostep edge, as explained by the model. An unbunched atomic step can be observed on one of the terraces. These residual atomic steps often divert the nanotubes from the nanostep edges (see SI).

For the graphoepitaxial formation of SWNTs along the faceted nanosteps we propose a wake-growth mechanism,⁵ where the catalyst slides along the inner and/or outer edges of the nanostep facets, leaving a nanotube on its trail. This mechanism, schematically implied in Figure 1d,g,i, is analogous to that previously proposed by us for the growth of SWNTs along atomic steps.⁵ To verify this mechanism with respect to a free growth mechanism², we repeated some of the experiments under a strong electric field perpendicular to the nanosteps and found that the growth direction is solely

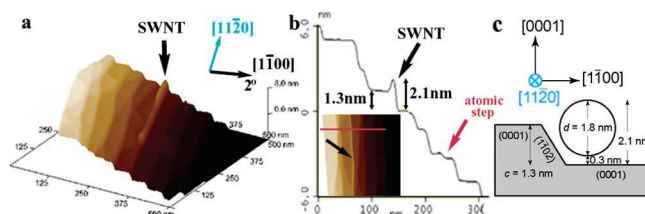


Figure 3. Topographic analysis of a graphoepitaxial SWNT (black arrows) on faceted nanosteps. (a) AFM 3D projection. (b) Height profile of a selected section (inset, red line). (c) Geometric model.

dictated by the nanosteps, unaffected by the electric field (see SI). The tendency of the nanotubes to grow along the faceted nanosteps may be attributed to a series of factors, including van der Waals interactions between the nanotubes and the nanosteps, which have similar sizes, electrostatic interactions between the facet edges and the nanotubes, and capillarity of the catalyst nanoparticles at the inner edge of the faceted nanosteps. In principle, faceted nanosteps could template the formation of periodic nanotube arrays. However, we note that the nanotube yield is lower on these annealed samples than on nonannealed ones. This may be attributed to the lower energy of the rearranged surface with respect to that of the atomic steps, which could stabilize the catalyst. Current efforts are underway to understand the mechanism of catalytic growth of SWNTs on these surfaces and the role of impurities, and to increase nanotube yield by varying the substrate, catalyst, and growth conditions.¹²

We propose that epitaxy, which has been so decisive in defining present technology, may also represent a powerful general approach for the long-sought bottom-up assembly of nanotube architectures for nanoelectronics and other applications. Previously reported lattice-oriented⁴ and atomic step-templated⁵ nanotube growth may be rationalized as nanotube-extended versions of incommensurate lattice-directed and ledge-directed epitaxy,¹³ respectively. Nanotube graphoepitaxy, presented here, would complete a set of epitaxial modes of nanotube growth, pointing to intriguing new possibilities in nanotechnology.

Acknowledgment. This research was supported by the U.S.-Israel Binational Science Foundation, the Israel Science Foundation, the Djanogly and the Alhadeff foundations. E.J. holds the Victor Erlich Career Development Chair.

Supporting Information Available: Experimental details, XRD data, and additional AFM images. This material is available free of charge via the Internet at <http://pubs.acs.org>.

References

- (1) Dresselhaus, M. S.; Dresselhaus, G.; Avouris, P. *Carbon Nanotubes: Synthesis, Properties and Applications*; Springer-Verlag: Berlin, 2001.
- (2) (a) Joselevich, E.; Lieber, C. M. *Nano Lett.* **2002**, *2*, 1137. (b) Ural, A.; Li, Y.; Dai, H. *Appl. Phys. Lett.* **2002**, *81*, 3464. (c) Radu, I.; Hanein, Y.; Cobden, D. *Nanotechnology* **2004**, *15*, 473.
- (3) Huang, S.; Cai, X.; Liu, J. *J. Am. Chem. Soc.* **2004**, *126*, 16698.
- (4) (a) Su, M.; Li, Y.; Maynor, B.; Buldum, A.; Lu, J. P.; Liu, J. *J. Phys. Chem B* **2000**, *104*, 6505. (b) Han, S.; Liu, X.; Zhou, C. *J. Am. Chem. Soc.* **2005**, *127*, 5294. (c) Ago, H.; Nakamura, K.; Ikeda, K.; Uehara, N.; Ishigami, N.; Tsuji, M. *Chem. Phys. Lett.* **2005**, *408*, 433.
- (5) Ismach, A.; Segev, L.; Wachtel, E.; Joselevich, E. *Angew. Chem., Int. Ed.* **2004**, *43*, 6140.
- (6) Shchukin, V. A.; Ledenstov, N. N.; Bimberg, D. *Epitaxy of Nanostructures*; Springer-Verlag: Berlin, 2004.
- (7) Smith, H. I.; Flanders, D. C. *Appl. Phys. Lett.* **1978**, *32*, 349.
- (8) Segalman, R. A.; Yokoyama, H.; Kramer, E. J. *Adv. Mater.* **2001**, *13*, 1152.
- (9) Choi, J. H.; Kim, D. Y.; Hockey, B. J.; Wiederhorn, S. M.; Handwerker, C. A.; Blendell, J. E.; Carter, W. C.; Roosen, A. R. *J. Am. Ceram. Soc.* **1997**, *80*, 62.
- (10) Heffelfinger, J. R.; Bench, M. W.; Carter, C. B. *Surf. Science* **1997**, *370*, L168.
- (11) Marchenko, V. I.; *Soviet Phys. JETP* **1981**, *54*, 605.
- (12) Hata, K.; Futaba, D. N.; Mizuno, K.; Namai, T.; Yumura, M.; Iijima, S. *Science* **2004**, *306*, 1362.
- (13) Hooks, D. E.; Fritz, T.; Ward, M. D. *Adv. Mater.* **2001**, *13*, 227.

JA052759M